Reference Submodule-Based Capacitor Monitoring Strategy for Modular Multilevel Converters

Deng, Fujin; Wang, Qingsong; Liu, Dong; Wang, Yanbo; Cheng, Ming; Chen, Zhe

Published in:
IEEE Transactions on Power Electronics

DOI (link to publication from Publisher):
10.1109/TPEL.2018.2857832

Publication date:
2019

Document Version
Accepted author manuscript, peer reviewed version

This article has been accepted for publication in a future issue of this journal, but has not been fully edited. Content may change prior to final publication. Citation information: DOI 10.1109/TPEL.2018.2857832, IEEE Transactions on Power Electronics

Reference Submodule-Based Capacitor Monitoring Strategy for Modular Multilevel Converters

Fujin Deng, *Member*, *IEEE*, Qingsong Wang, *Senior Member*, *IEEE*, Dong Liu, *Member*, *IEEE*, Yanbo Wang, *Member*, *IEEE*, Ming Cheng, *Fellow*, *IEEE*, Zhe Chen, *Senior Member*, *IEEE*

***Abstract*--The modular multilevel converter (MMC) is attractive for medium or high-power applications because of the advantages of its high modularity, availability, and high power quality. Reliability is one of the most important challenges for the MMC consisting of a large number of submodules (SMs). The capacitor monitoring is one of the important issues in the MMC. This paper proposed a reference submodule (RSM)-based capacitor monitoring strategy for the capacitance estimation in the MMC, where the capacitances in the monitoring SMs can be estimated based on the capacitor voltage relationship between the RSM and the monitoring SMs. The proposed monitoring strategy does not rely on the information of all capacitor voltage and current, which effectively simplifies the algorithm for capacitance estimation. The simulation studies with the time-domain professional tool PSCAD/EMTDC are conducted and a down-scale MMC prototype is also tested in the laboratory with the proposed capacitor monitoring strategy. The study results confirm the effectiveness of the proposed capacitor monitoring strategy.**

***Index Terms*— Capacitor, modular multilevel converters (MMCs), monitoring, submodule.**

I. Introduction

Modular multilevel converters (MMCs) have been regarded as one of the most competitive converters for medium to high-voltage high-power applications with the advantages such as the excellent output voltage waveforms, very high efficiency [1, 2], etc. A multilevel voltage can be produced with the flexible operation of the MMC while reducing average switching frequency without compromising the power quality [3, 4]. Recently, due to the easy construction, assembling, and flexibility in converter design, the MMC becomes promising for various applications such as machine drives [5], electric railway supplies [6] and microgrid [7].

This work was supported in part by the Natural Science Foundation of Jiangsu Province under Project BK20170675.

Fujin Deng, Qingsong Wang and Ming Cheng are with the School of Electrical Engineering, Southeast University, Nanjing, 210096, China (fdeng@seu.edu.cn, qswang@seu.edu.cn, mcheng@seu.edu.cn)

Dong Liu, Yanbo Wang and Zhe Chen are with the Department of Energy Technology, Aalborg University, Aalborg, 9220 Denmark (dli@et.aau.dk, ywa@et.aau.dk, zch@et.aau.dk).

Reliability is one of the most important challenges for the MMC. The MMC consists of a large number of devices (e.g. switch, diode and capacitor) and each device can be considered as a potential failure point [8, 9]. Recently, a number of studies about the switch and diode faults in the MMC have been reported. The sliding mode observer [10], Kalman filter [11], state observer [12], etc. are employed in the MMC. Through the comparison between the estimated values and the measured values, the switch open-circuit fault is detected. A resilient framework is presented for fast fault diagnosis and restoration about the switch open-circuit faults in the MMC [13]. The clustering algorithm based method and a calculated capacitance based method are introduced for detecting the switch open-circuit faults [14]. The supervisory sensor is presented in the MMC, where the switch fault can be diagnosed by comparing the output voltages of a set of submodules (SMs) [15]. A varistor-based SM configuration is presented for the fault diagnosis and protection under the diode open-circuit faults in the MMC [16].

The electrolytic capacitor is widely considered for the MMC in some applications such as motor drive and microgrid [5], [7], [17-21] based on its feature such as high capacitance per unit volume. Due to the chemical process, aging effect, etc., the capacitor in the MMC would gradually deteriorate, which is normally expressed by the capacitance drop [22-24]. Normally, the deteriorated capacitor needs be replaced when its capacitance drops below the threshold value, such as 80% of the rated value [22]. As a consequence, the MMC has to work with the different capacitances in the different SMs, which would affect the performance of the MMC [25]. Therefore, an effective capacitor monitoring method to estimate the capacitance is essential for the MMC, from which a predictive maintenance is possible, leading to the better reliability of the MMC.

Several studies have been presented for the capacitor condition monitoring. Reference [22] presented a condition monitoring scheme for capacitors in the MMC, where the capacitance in the SM is estimated by a recursive least square algorithm based on the capacitance estimation using the information of the capacitor voltage, arm current and SM switching state. However, an ac current is required to be injected into the circulating current, which increases capacitor

This article has been accepted for publication in a future issue of this journal, but has not been fully edited. Content may change prior to final publication. Citation information: DOI 10.1109/TPEL.2018.2857832, IEEE Transactions on Power Electronics

voltage ripple and affects MMC performance. Reference [23] employed a Kalman filter algorithm to estimate the SM capacitance in the MMC, which estimates the capacitance based on the capacitor voltage and current. However, the Kalman filter algorithm complicates the capacitance estimation. Reference [24] presented a simple capacitor monitoring algorithm, which can estimate the capacitances in the SMs based on the relationship between the arm average capacitance and the capacitance in each SM of the arm. However, the above methods need to monitor all SMs' switching states for calculating the capacitor current and estimate all SMs' capacitances based on the integral computation, which complicate the capacitor monitoring algorithm.

In this paper, a reference submodule (RSM)-based capacitor monitoring strategy is proposed. Based on the capacitor voltage relationship between the RSM and the monitoring SMs, the capacitance in the monitoring SMs can be estimated with simple algorithm. The proposed strategy does not rely on the information of all capacitor voltage and current for capacitance estimation, which effectively simplifies the computation in comparison with the aforementioned methods [22-24].

This paper is organized as follows. Section II presented the operation of the MMC. Section III proposed the RSM-based capacitor monitoring for the MMC. The system simulation and experimental tests are presented in Sections IV and V, respectively, to show the effectiveness of the proposed capacitor monitoring strategy. Finally, the conclusions are presented in Section VI.

II. Operation Principle of MMCs

A. Structure of MMCs

A three-phase MMC is shown in Fig. 1(a), which contains six arms. Each arm consists of n identical SMs and an arm inductor L_s. Fig. 1(b) shows the i-th SM (i=1, 2……n) in the upper arm of phase A, which contains the switch/diode T_t/D_t, T_b/D_b and a dc capacitor C_{aui} [26]. The SM is normally controlled with a switching function S_{aui} as

$$S_{aui}=\begin{cases}1, & T_t \text{ is on and } T_b \text{ is off}\\ 0, & T_t \text{ is off and } T_b \text{ is on}\end{cases} \tag{1}$$

The SM output voltage u_{aui} is

$$u_{aui}=S_{aui}\cdot u_{caui} \tag{2}$$

where u_{caui} is the capacitor voltage. Table I shows the two states of the SM. One is "On" state under S=1, where u_{aui} equals u_{caui}. The other one is "Off" state under S=0, where u_{aui} equals 0. In the "On" state, the charge and discharge of the capacitor C_{aui} depends on the arm current flow direction. If the arm current i_{ua} is positive, as shown in Fig. 1(a), the capacitor in the on-state SM would be charged and u_{caui} is increased. If the arm current i_{ua} is negative, the capacitor in the on-state SM would be discharged and u_{caui} is decreased. In the "Off" state, the SM capacitor would be bypassed and u_{caui} is unchanged, irrespective of the arm current flow direction [27].

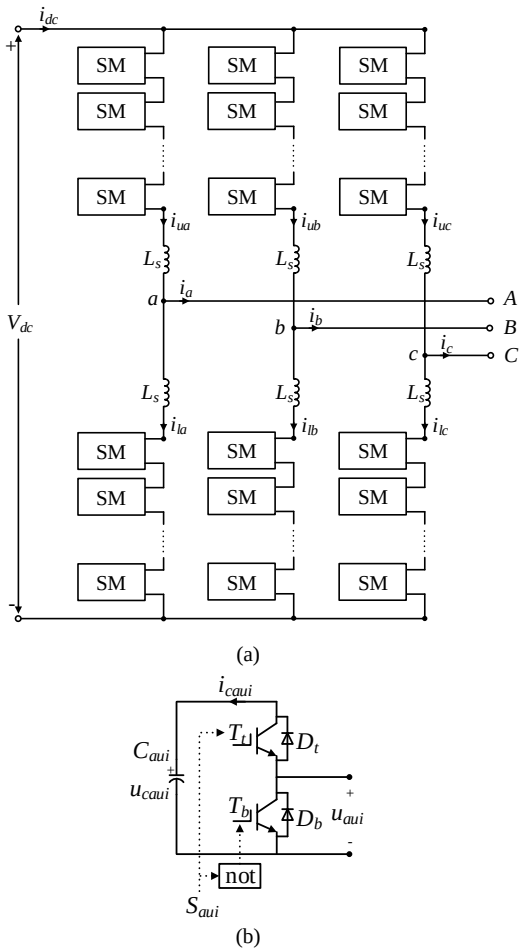

Fig. 1. (a) Block diagram of a three-phase MMC. (b) SM unit.

TABLE I
Operation of the SM

SM state	S_{aui}	T_t	T_b	u_{aui}	Arm current i_{ua}	C_{aui}	u_{caui}
On	1	On	On	u_{caui}	u_c	Charge	Increased
					0	Bypass	Unchanged
Off	0	Off	Off	0	u_c	Discharge	Decreased

In Fig. 1, the upper and lower arm current i_{uj} and i_{lj} (j=a, b, c) can be described as

$$\begin{cases} i_{uj}=\dfrac{i_j}{2}+i_{diff\_j} \\ i_{lj}=-\dfrac{i_j}{2}+i_{diff\_j}\end{cases} \tag{3}$$

with

$$i_{diff\_j}=\frac{i_{dc}}{3}+i_{2f\_j} \tag{4}$$

where i_j is the ac grid current of phase j. i_{diff_j} is the inner difference current of phase j, which contains two parts and can be expressed as (4) [28]. One part is the dc component, i_{dc}/3. The other part is the circulating current i_{2f_j} of phase j.

B. Voltage-Balancing Control of MMCs

The conventional voltage-balancing control (C-VBC) of the MMC is shown in Fig. 2 (a). Under the modulation schemes, through the comparison between the reference signal and the carriers, the number n_{on} of the on-state SMs can be obtained.

This article has been accepted for publication in a future issue of this journal, but has not been fully edited. Content may change prior to final publication. Citation information: DOI 10.1109/TPEL.2018.2857832, IEEE Transactions on Power Electronics

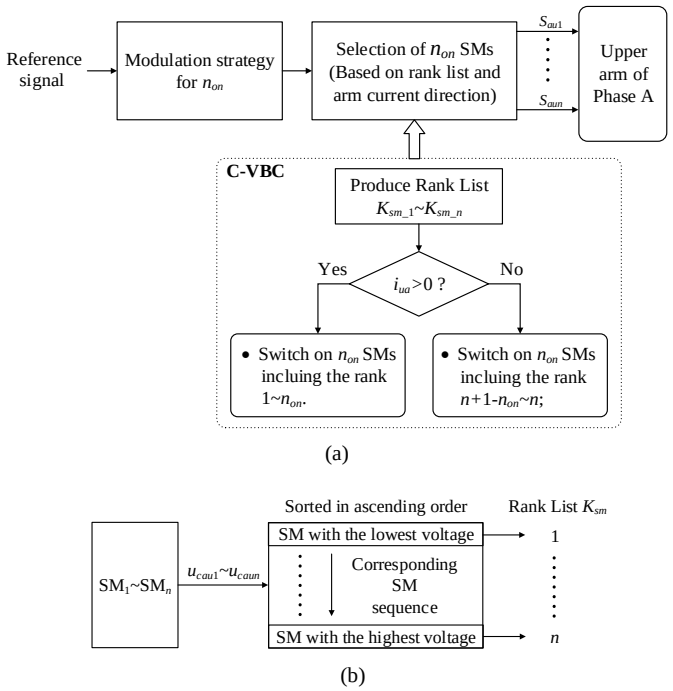

Fig. 2 (a) C-VBC for MMCs. (b) Rank list production.

The switching function for each SM can be decided based on n_{on}, the rank list and the arm current. Fig. 2(b) shows the production of the rank list. The capacitor voltage u_{cau1}~u_{caun} in the arm is measured and the SMs in the arm are ordered according to their capacitor voltage in ascending order. And then, the rank K_{sm_i} (i=1, 2…n) corresponding to the SM$_i$ in the arm can be produced, where the K_{sm} for the SM with the lowest voltage is 1 and the K_{sm} for the SM with the highest voltage is n. If the arm current is positive, the n_{on} SMs with the lowest voltage corresponding to the rank 1~n_{on} will be switched on. If the arm current is negative, the n_{on} SMs with the highest voltage corresponding to the rank n-n_{on}+1~n will be switched on, which ensures the capacitor voltage balancing in the arm [29].

III. Proposed RSM-Based Capacitor Monitoring Strategy

A. Conventional Capacitor Monitoring Method

In the conventional capacitor monitoring for the MMC [22, 23], the capacitance C_{aui} shown in Fig. 1(b) can be directly estimated based on the arm current i_{ua}, capacitor voltage u_{caui} and the switching function S_{aui} as

$$C_{aui} = \frac{1}{u_{caui}} \int S_{aui} \cdot i_{ua} dt \tag{5}$$

The capacitance estimation in the conventional method can be achieved with very high accuracy, and the error is less than about 1%. However, the conventional method not only needs the information of all capacitor voltage and current, but also relies on the complex integral computation. If all capacitances in the arm are estimated by the conventional monitoring method, it would complicate the algorithm and increase the computation burden.

B. Proposed RSM-Based Capacitor Monitoring Method

In order to simplify capacitor monitoring algorithm, the RSM-based capacitor monitoring method is proposed for the capacitance estimation in the arm, as shown in Fig. 3. In the proposed RSM-based capacitor monitoring method, some SM is selected as the RSM and the capacitances in the other SMs can be estimated based on the capacitance in the RSM.

Suppose that the capacitance in the RSM has been estimated, in order to monitor the capacitance C_{aui} in the SM$_i$, $i \in (1, 2, \ldots n)$, the switching function S_{rsm} for the RSM must be the same to S_{aui} for the SM$_i$, as S_{rsm}=S_{aui}. In this situation, the RSM capacitor voltage u_{rsm} and the SM$_i$ capacitor voltage u_{caui} can be expressed as

$$\begin{cases} u_{rsm} = \dfrac{1}{C_{rsm}} \int S_{rsm} \cdot i_{ua} dt \\ u_{caui} = \dfrac{1}{C_{aui}} \int S_{rsm} \cdot i_{ua} dt \end{cases} \tag{6}$$

According to (6), the relationship between the capacitance C_{rsm} and C_{aui} can be obtained as

$$C_{aui} = C_{rsm} \frac{\Delta u_{rsm}}{\Delta u_{caui}} \tag{7}$$

where Δu_{rsm} and Δu_{caui} are the peak-to-peak values of the voltage u_{rsm} and u_{caui}, respectively, as shown in Fig. 3.

According to (7), the capacitance C_{aui} can be estimated in one fundamental period based on the measured RSM capacitor voltage u_{rsm}, the measured SM$_i$ capacitor voltage u_{caui} and the estimated RSM capacitance C_{rsm}, as shown in Fig. 3.

C. Proposed CM-VBC

To realize the proposed RSM-based capacitor monitoring shown in Fig. 3, a capacitor monitoring-based voltage-balancing control (CM-VBC) is proposed to select n_{on} on-state SMs, as shown in Fig. 4. The proposed CM-VBC not only balances the capacitor voltages in the arm for ensuring the normal operation of the MMC, but also ensures that the S_{rsm} for the RSM follows the S_{aui} for the monitoring SM$_i$, so as to complete the proposed RSM-based capacitor monitoring.

In Fig. 4, the n-1 SMs in the arm except RSM are sorted based on their capacitor voltages in the ascending order, so as to produce the rank K_{sm} for the corresponding SM. Suppose that the SM$_i$ corresponding to the rank K_{sm_i} is to be monitored, the selection of n_{on} on-state SMs will be decided based on the arm current i_{ua} and the ranks of the n-1 SMs, as follows.

1) i_{ua} > 0 & K_{sm_i} < n_{on}: the n_{on}-1 SMs corresponding to the rank 1~n_{on}-1 are switched on. In addition, the RSM is also switched on. In this situation, SM$_i$ and RSM are both switched on.
2) i_{ua} > 0 & K_{sm_i} = n_{on}: the n_{on}-1 SMs corresponding to the rank 1~n_{on}-2 and n_{on} are switched on. In addition, the RSM is also switched on. Here, SM$_i$ and RSM are both switched on.
3) i_{ua} > 0 & K_{sm_i} > n_{on}: the n_{on} SMs corresponding to the rank 1~n_{on} are switched on. In this situation, SM$_i$ and RSM are both switched off.

This article has been accepted for publication in a future issue of this journal, but has not been fully edited. Content may change prior to final publication. Citation information: DOI 10.1109/TPEL.2018.2857832, IEEE Transactions on Power Electronics

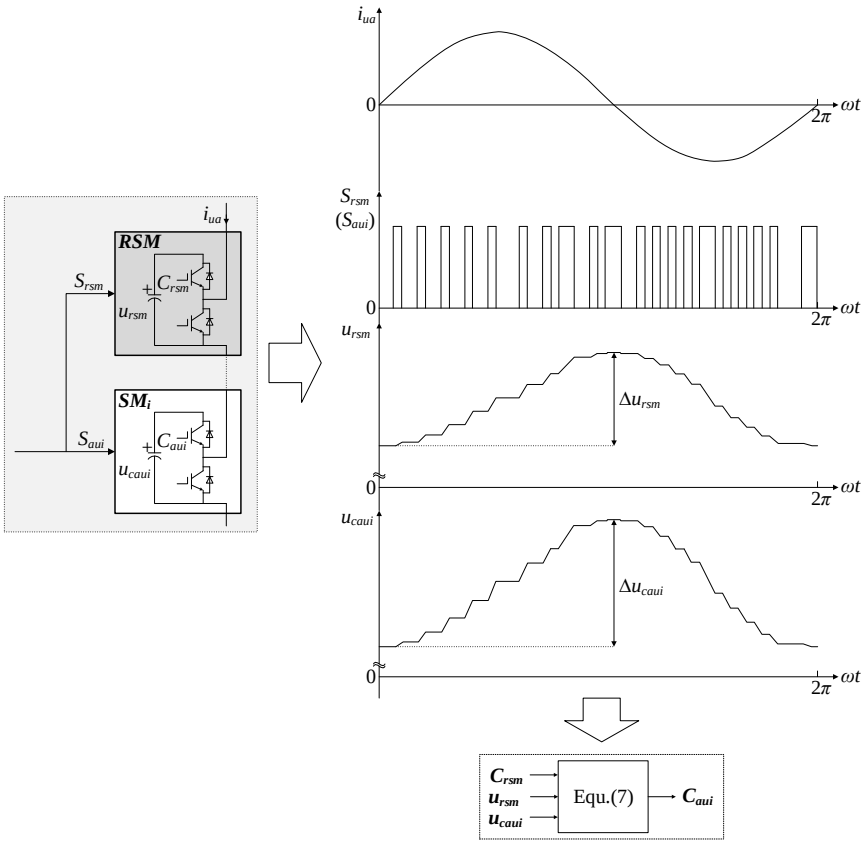

Fig. 3. Proposed RSM-based capacitor monitoring method.

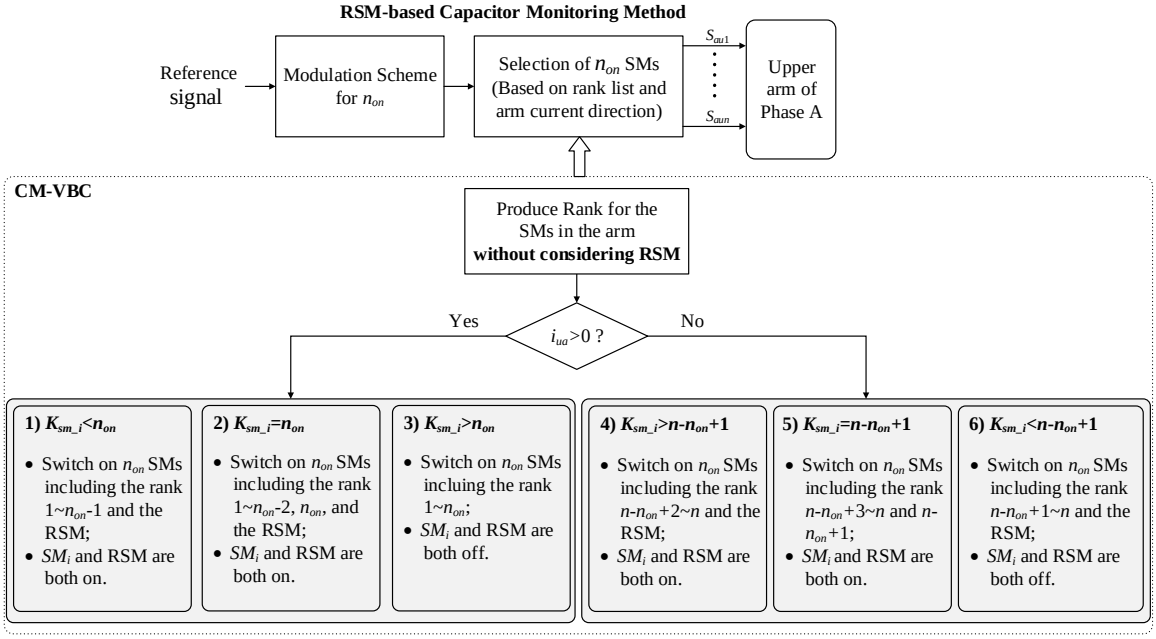

Fig. 4. Proposed CM-VBC for RSM-based capacitor monitoring.

4) $i_{ua} < 0$ & $K_{sm\_i} > n\text{-}n_{on}\text{+}1$: the n_{on}-1 SMs corresponding to the rank $n\text{-}n_{on}\text{+}2\sim n$ are switched on. In addition, the RSM is also switched on. Here, SM_i and RSM are both switched on.
5) $i_{ua} < 0$ & $K_{sm\_i} = n\text{-}n_{on}\text{+}1$: the n_{on}-1 SMs corresponding to the rank $n\text{-}n_{on}\text{+}3\sim n$ and $n\text{-}n_{on}\text{+}1$ are switched on. In addition, the RSM is also switched on. In this situation, SM_i and RSM are both switched on.
6) $i_{ua} < 0$ & $K_{sm\_i} < n\text{-}n_{on}\text{+}1$: the n_{on} SMs corresponding to the rank $n\text{-}n_{on}\text{+}1\sim n$ are switched on. Here, SM_i and RSM are both switched off.

D. Selection of RSM

In the proposed CM-VBC, although the capacitor voltages in the arm are kept balanced, the peak-to-peak value Δu_{rsm} in u_{rsm} would be variable, as shown in Fig. 3, which depends on

This article has been accepted for publication in a future issue of this journal, but has not been fully edited. Content may change prior to final publication. Citation information: DOI 10.1109/TPEL.2018.2857832, IEEE Transactions on Power Electronics

the relationship between C_{rsm} and C_{aui} shown in (7). If C_{rsm} is bigger than C_{aui}, Δu_{rsm} is smaller than Δu_{caui}. In addition, the bigger of C_{rsm}, the smaller of Δu_{rsm}. If C_{rsm} is smaller than C_{aui}, Δu_{rsm} is bigger than Δu_{caui}. The smaller of C_{rsm}, the bigger of Δu_{rsm}, as shown in Table II.

TABLE II
VOLTAGE RIPPLE IN RSM

RSM's Capacitance C_{rsm}	RSM's voltage ripple Δu_{rsm}
$> C_{aui}$	$< \Delta u_{caui}$
$< C_{aui}$	$> \Delta u_{caui}$

Based on above analysis, the RSM should be selected with the SM, whose capacitance is the biggest one among C_{au1}~C_{aun}. It ensures that the Δu_{rsm} is always not bigger than the peak-to-peak value of the other SMs' capacitor voltages, which reduces the capacitor voltage ripple in the RSM.

Suppose that the electrolytic capacitor is used in the MMC and the capacitor needs to be replaced when its capacitance drops to 80% of the rated value, the RSM's Δu_{rsm} would be reduced by 0.2 p.u. at most. On the other hand, the capacitor voltages in the arm are kept balanced with the CM-VBC. Although the peak-to-peak value Δu_{rsm} of the RSM's capacitor voltage is less than that of the other SMs' capacitor voltages during the capacitor monitoring period, the capacitor voltage's peak-to-peak value is far less than the capacitor voltage [1-10], and therefor the impact of the variable RSM's Δu_{rsm} on the MMC performance during the capacitor monitoring period can be omitted.

E. Proposed Capacitor Monitoring Strategy

Based on above analysis, the capacitor monitoring strategy is proposed, as shown in Fig. 5, which estimates the SM's capacitances in the sequence from SM1 to SM*n* round. Firstly, the SM1 is selected as the RSM, and the RSM capacitance is estimated based on the conventional method as (5). Based on the RSM, the capacitance in the SM2 is estimated with the RSM-based monitoring method as shown in Fig. 6.

In Fig. 6, the selection signal (*SS*) is initially "0" and the C-VBC is enabled, where u_{cau1}~u_{caun} are kept the same with each other. When the capacitor in the SM2 is demanded to be monitored, the *SS* is switched to "1" and the RSM-based CM-VBC is enabled for one fundamental period. Here, the RSM's Δu_{rsm} would be changed, which is used for the SM2 capacitor monitoring based on (7). Afterwards, the *SS* is switched back to "0" again to keep the u_{cau1}~u_{caun} the same with each other, which waits for the next command to monitor the capacitance in the other SMs.

After the capacitance in SM2 is estimated, the RSM will be updated. Among the estimated SMs, the SM with the biggest capacitance is selected as the RSM. Afterwards, the SM3, SM4……will be monitored with the same method, which is not repeated here.

Although, the capacitor voltage ripple of the RSM is a little smaller than those of the other SMs in the CM-VBC, the capacitor voltage ripple is far less than the capacitor voltage, which makes that the proposed capacitor monitoring has little effect on the performance of the MMC. In addition, due to the chemical process and aging effect, the speed of the capacitance drop is quite slow. Therefore, the SM capacitors in the arm can be monitored in the sequence from SM1 to SM*n* round with some short interval such as one fundamental period.

One thing to be mentioned is that, the capacitor monitoring in the proposed strategy is indirectly realized based on the SM1's capacitance, as shown in Fig. 5. Hence, the estimation accuracy of the SMs' capacitor depends on that of the SM1's capacitance. According to [22, 23], the SM1's capacitance can be estimated by (5) with very high accuracy, and the error is less than about 1%, which guarantees the capacitance estimation accuracy in the proposed strategy. On the other hand, in order to ensure the high estimation accuracy, the selected RSM's capacitor will be estimated by (5) at an interval of time *T*, as shown in Fig. 5.

From Fig. 5, it can be observed that the proposed capacitor monitoring method does not rely on the information of all capacitors' voltage and current for the complicated integral computation, which effectively simplifies the capacitor monitoring algorithm.

IV. SIMULATION STUDIES

To verify the proposed strategy, a three-phase MMC system shown in Fig. 7 is simulated with the time-domain simulation tool PSCAD/EMTDC. In the simulation, the active power *P* and the reactive power *Q* is 100 MW and 0 MVar, respectively. The capacitances C_{au2}~C_{au6} drop, where C_{au2}=13.5 mF, C_{au3}=12 mF, C_{au4}=10.5 mF, C_{au5}=9 mF, C_{au6}=7.5 mF, respectively. The other system parameters are shown in the Table III.

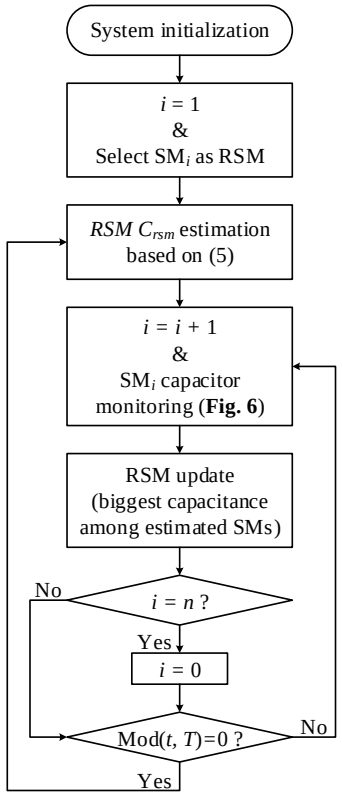

Fig. 5. Flowchart of the proposed capacitor monitoring strategy for MMCs.

This article has been accepted for publication in a future issue of this journal, but has not been fully edited. Content may change prior to final publication. Citation information: DOI 10.1109/TPEL.2018.2857832, IEEE Transactions on Power Electronics

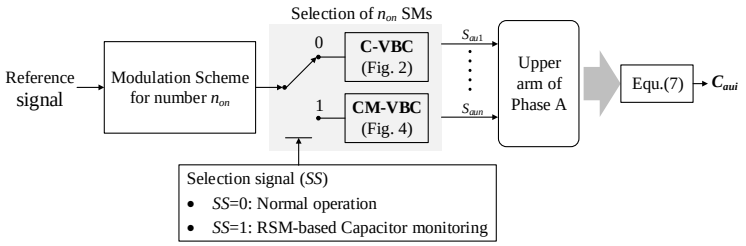

Fig. 6. Proposed capacitor monitoring.

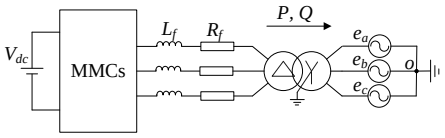

Fig. 7. Block diagram of the simulation system.

TABLE III
SIMULATION SYSTEM PARAMETERS

Parameters	Value
DC-link voltage V_{dc} (kV)	100
Grid line-to-line voltage (kV)	220
Grid frequency (Hz)	50
Transformer voltage rating	50 kV/220 kV
Transformer leakage reactance	10%
Number of SMs per arm n	100
Nominal SM capacitance C (mF)	15
Inductance L_s (mH)	10
Load inductance L_f (mH)	2

Fig. 8 shows the performance of the MMC with the proposed capacitor monitoring strategy, where the average switching frequency is about 2.5 kHz. Fig. 8(a) shows the arm current i_{ua} and i_{la}. Fig. 8(b) shows capacitor voltage u_{cau1}~u_{cau10}. Before 1.8 s, the C-VBC is used with "*SS*=0". With the conventional capacitor monitoring method, the C_{au1} is estimated as 15 mF, as shown in Fig. 8(c). And then, the SM_1 is selected as the RSM. Between 1.8 s and 1.82 s, the C_{au2} is monitored with "*SS*=1", where the switching function for SM_1 is the same to that for SM_2. The different C_{au1} and C_{au2} result in the different capacitor voltage u_{cau1} and u_{cau2}, as shown in Fig. 8(e), where Δu_{cau1} and Δu_{cau2} are 0.126 and 0.139, respectively. According to (7), the capacitor C_{au2} is monitored as 13.5 mF shown in Fig. 8(c). And then, the MMC goes back to the C-VBC with "*SS*=0", where all capacitor voltage are kept the same again between 1.82 s and 1.84 s. Similarly, the C_{au3}, C_{au4}, C_{au5} and C_{au6} are monitored with "*SS*=1" one after another. In Fig. 8(f), C_{au3} is monitored as 12 mF with Δu_{cau1}=0.111 and Δu_{cau3}=0.139. In Fig. 8(g), C_{au4} is monitored as 10.5 mF with Δu_{cau1}=0.098 and Δu_{cau4}=0.139. In Fig. 8(h), C_{au5} is monitored as 9 mF with Δu_{cau1}=0.084 and Δu_{cau5}=0.139. In Fig. 8(i), C_{au6} is monitored as 7.5 mF with Δu_{cau1}=0.07 and Δu_{cau6}=0.139. Owing to that C_{au1} is the biggest among C_{au1}~C_{au6}, the SM_1 is always selected as the RSM and Δu_{cau1} is less than Δu_{cau2}~Δu_{cau6}, as shown in Fig. 8(b).

Fig. 9 shows the THD of the arm current i_{ua} when the proposed strategy is employed to estimate the capacitances in the SM1~SM6, respectively, where the average switching frequency is about 2.5 kHz. In Fig. 9, the THDs of i_{ua} are almost the same with each other. It shows that the variable RSM capacitor voltage ripple has little impact on the MMC performance in the proposed capacitor monitoring strategy.

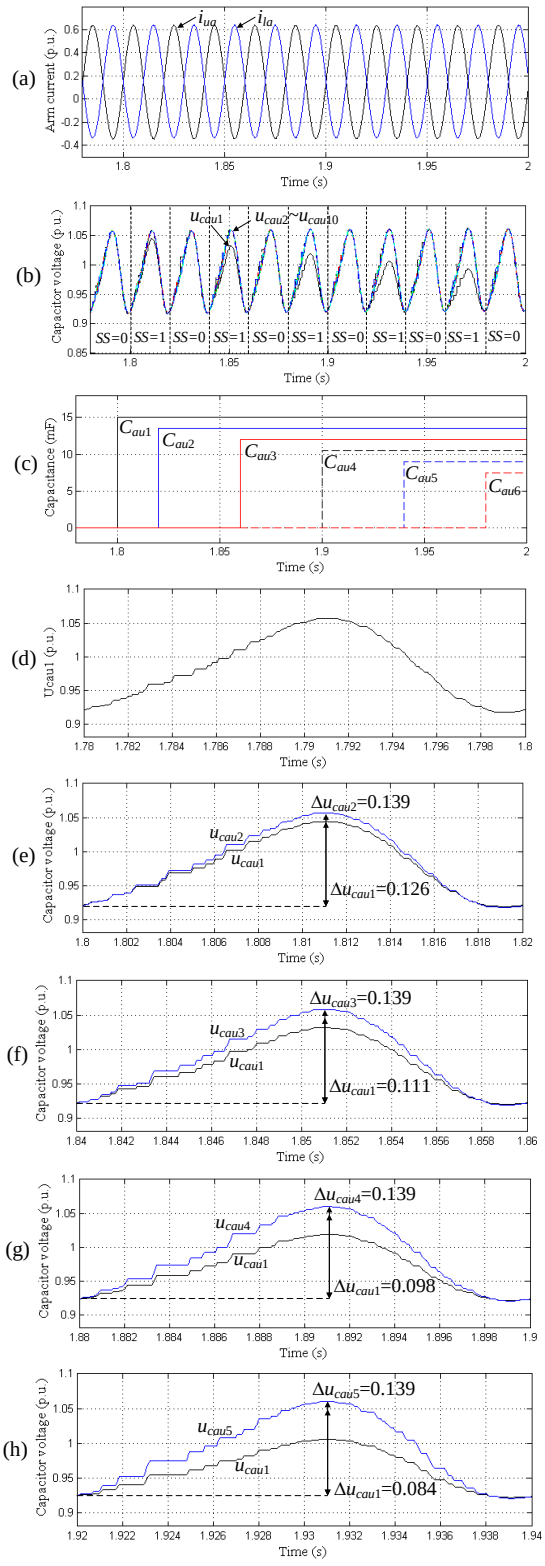

This article has been accepted for publication in a future issue of this journal, but has not been fully edited. Content may change prior to final publication. Citation information: DOI 10.1109/TPEL.2018.2857832, IEEE Transactions on Power Electronics

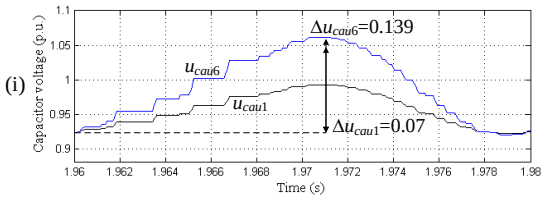

Fig. 8. (a) i_{ua} and i_{la}. (b) Upper arm capacitor voltage u_{cau1}~u_{cau10}. (c) Calculated capacitance C_{au1}~C_{au6}. (d) u_{cau1}. (e) u_{cau1} and u_{cau2}. (f) u_{cau1} and u_{cau3}. (g) u_{cau1} and u_{cau4}. (h) u_{cau1} and u_{cau5}. (i) u_{cau1} and u_{cau6}.

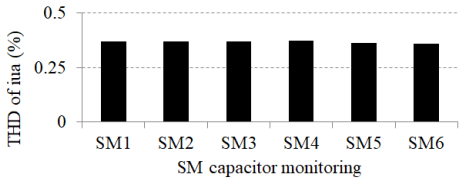

Fig. 9. THD analysis of i_{ua}.

Fig. 10 shows the performance of the MMC with the proposed capacitor monitoring strategy, where the average switching frequency is about 600 Hz. Fig. 10(a) shows the arm current i_{ua} and i_{la}. Fig. 10(b) shows capacitor voltage u_{cau1}~u_{cau10}. With the proposed capacitor monitoring method, the capacitors C_{au1}, C_{au2}, C_{au3}, C_{au4}, C_{au5} and C_{au6} are monitored as 15 mF, 13.5 mF, 12 mF, 10.5 mF, 9 mF and 7.5 mF, respectively, as shown in Figs. 10(c)~(i).

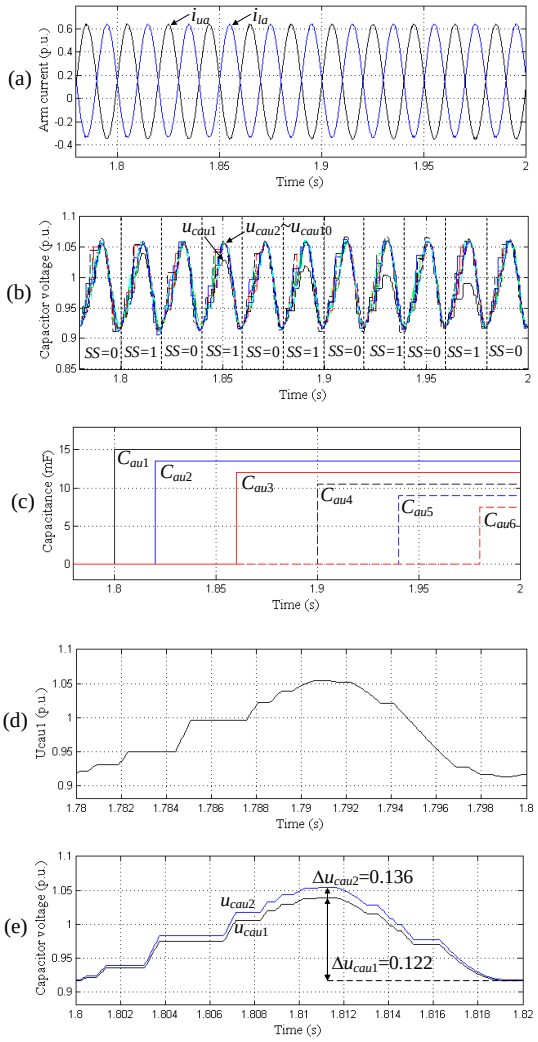

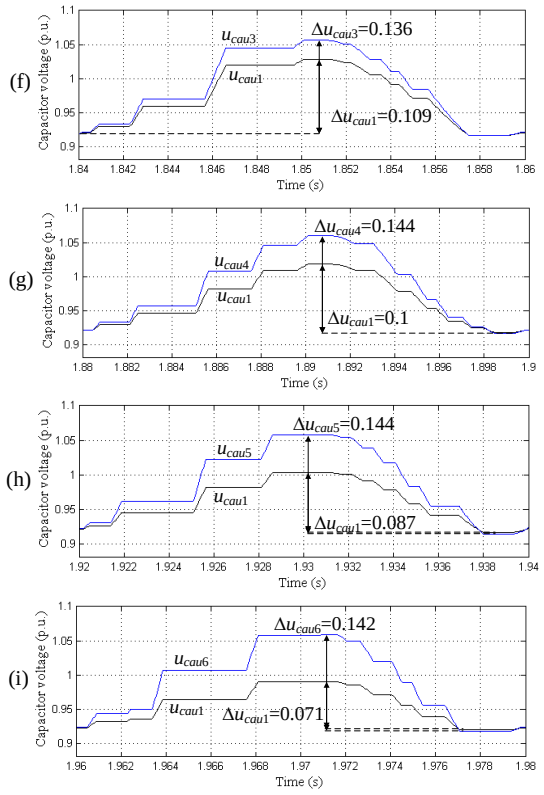

Fig. 10. (a) i_{ua} and i_{la}. (b) Upper arm capacitor voltage u_{cau1}~u_{cau10}. (c) Calculated capacitance C_{au1}~C_{au6}. (d) u_{cau1}. (e) u_{cau1} and u_{cau2}. (f) u_{cau1} and u_{cau3}. (g) u_{cau1} and u_{cau4}. (h) u_{cau1} and u_{cau5}. (i) u_{cau1} and u_{cau6}.

Fig. 11 shows the THD of the arm current i_{ua} when the proposed strategy is employed to estimate the capacitances in the SM1~SM6, respectively, where the average switching frequency is about 600 Hz. It can be observed that the THDs are almost close to each other, which shows that the variable RSM capacitor voltage ripple has little impact on the MMC performance in the proposed capacitor monitoring strategy.

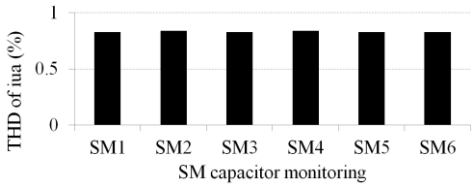

Fig. 11. THD analysis of i_{ua}.

V. Experimental Studies

A single-phase MMC prototype with 7 SMs per arm, as shown in Fig. 12(a), is built in the laboratory to confirm the proposed scheme. Fig. 12(b) shows the photo of the experimental setup. A three-phase uncontrolled rectifier with electrolytic capacitors constitutes the dc bus voltage. The IXFK48N60P is used as the switch/diode in each cell. The system control algorithm is implemented in dSPACE DS1005 and the pulse signals from the dSPACE are transferred to the driving panel of each SM by optical fiber. The system parameters are shown in the Table IV. To verify the proposed capacitor monitoring strategy, the small capacitor C_{au2} and C_{au3} are used, whose manufacture parameters are 1.88 mF and 1.41 mF, respectively.

This article has been accepted for publication in a future issue of this journal, but has not been fully edited. Content may change prior to final publication. Citation information: DOI 10.1109/TPEL.2018.2857832, IEEE Transactions on Power Electronics

TABLE IV
EXPERIMENTAL SYSTEM PARAMETERS

Parameters	Value
DC-link voltage V_{dc} (V)	280
Rated frequency (Hz)	50
Capacitor C_{in} (mF)	2.2
Nominal capacitor C_{sm} (mF)	2.35
Inductor L_s (mH)	3
Load inductor L (mH)	1.8
Load resistor R (Ω)	10
Switching frequency (kHz)	5

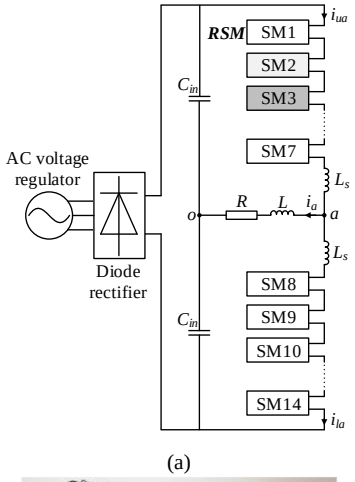

(a)

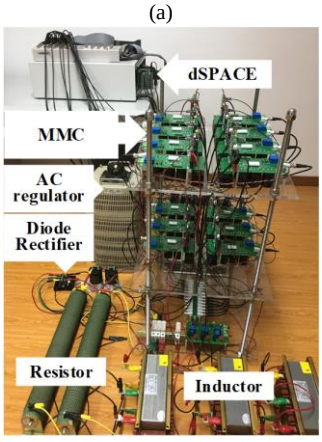

(b)

Fig. 12. (a) Experimental circuit. (b) Photo of the experimental system.

Fig. 13 shows the performance of the MMC under the proposed capacitor monitoring strategy. Fig. 13(a) shows the arm current i_{ua}. Fig. 13(b) shows the capacitor voltage u_{cau1}, u_{cau2} and u_{cau3} in SM1, SM2 and SM3, respectively. Before 0.02 s, the C-VBC is used with "*SS*=0". With the conventional capacitor monitoring method, the C_{au1} in SM1 is obtained as 2.22 mF. And then, the SM1 is selected as the RSM. Between 0.02 s and 0.04 s, the capacitor C_{au2} in SM2 is monitored with "*SS*=1", as shown in Fig. 13(c), where Δu_{cau1}=4.01 V and Δu_{cau2}=5.03 V. Consequently, the C_{au2} in SM2 is obtained as 1.77 mF based on (7). Between, 0.04 s and 0.06 s, the C-VBC is enabled to keep the capacitor voltage the same with "*SS*=0". Afterwards, the capacitor C_{au3} in SM3 is monitored with "*SS*=1" between 0.06 s and 0.08 s, as shown in Fig. 13(d), where Δu_{cau1}=3.09 V and Δu_{cau3}=5.13 V. As a result, the C_{au3} in SM3 is obtained as 1.34 mF based on (7). Owing to that C_{au1} is the biggest among C_{au1}~C_{au3}, the SM_1 is always selected as the RSM and Δu_{cau1} is less than Δu_{cau2} and Δu_{cau3}, as shown in Figs. 13(b)~(d).

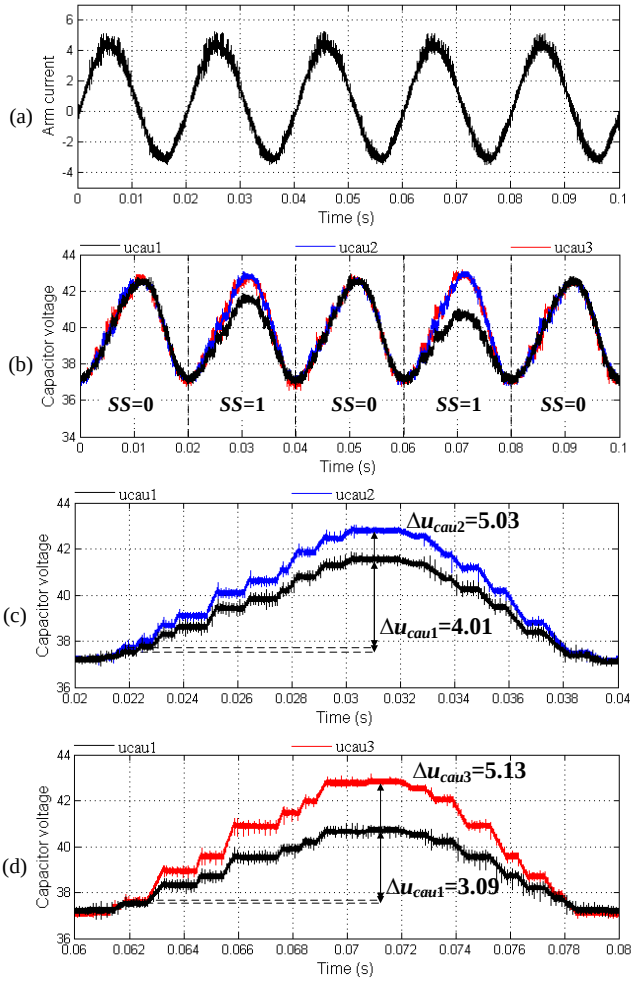

Fig. 13. (a) i_{ua}. (b) u_{cau1}~u_{cau3}. (c) u_{cau1} and u_{cau2}. (d) u_{cau1} and u_{cau3}.

Fig. 14(a) shows the monitored capacitance with the proposed strategy and the measured capacitance with the UNI-T UT612 LCR meter at 100 Hz and 25°C. Fig. 14(b) shows the errors between the estimated capacitance and the measured capacitance. It shows small error, where the maximum error is less than 0.52%.

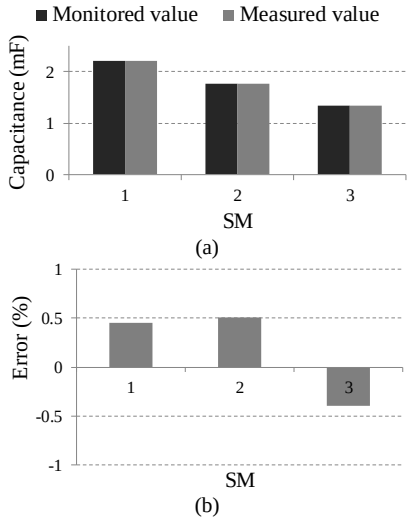

Fig. 14. (a) Monitored capacitance and measured capacitance. (b) Error.

This article has been accepted for publication in a future issue of this journal, but has not been fully edited. Content may change prior to final publication. Citation information: DOI 10.1109/TPEL.2018.2857832, IEEE Transactions on Power Electronics

Fig. 15 shows the THD of the arm current i_{ua} when the proposed strategy is employed to estimate the capacitances in the SM1~SM3, respectively, where the THDs are almost the same with each other. It shows that the variable RSM capacitor voltage ripple has little impact on the MMC performance in the proposed capacitor monitoring strategy.

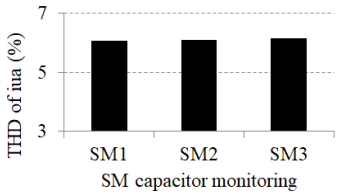

Fig. 15. THD analysis of i_{ua}.

VI. Conclusions

In this paper, a RSM-based capacitor monitoring strategy is proposed for the MMC. The SM with the biggest capacitance is selected as the RSM. Under the proposed capacitor monitoring-based voltage-balancing control, the peak-to-peak value of the RSM's capacitor voltage would be variable. Based on the capacitor voltage relationship among the RSM and the monitoring SMs, the SMs' capacitances can be estimated based on the RSM's capacitance. The proposed RSM-based capacitor monitoring strategy does not rely on the information of all capacitor voltage and current, which realizes the capacitor monitoring with simple algorithm and simplify the computation. The simulation and experiment studies are conducted to verify the proposed strategy, and the results show the effectiveness of the proposed RSM-based capacitor monitoring strategy.

References

[1] S. Debnath, J. Qin, B. Bahrani, M. Saeedifard, and P. Barbosa, "Operation, control, and applications of the modular multilevel converter: a review," *IEEE Trans. Power Electron.*, vol.30, no. 1, pp. 37-53, Jan. 2015.

[2] M. A. Perez, S. Bernet, J. Rodriguez, S. Kouro, and R. Lizana, "Circuit topologies, modeling, control schemes, and applications of modular multilevel converters," *IEEE Trans. Power. Electron.*, vol. 30, no. 1, pp. 4-17, Jan. 2015.

[3] A. Dekka, B. Wu, R. L. Fuentes, M. Perez and N. R. Zargari, "Evolution of Topologies, Modeling, Control Schemes, and Applications of Modular Multilevel Converters," *IEEE J. Emerg. Sel. Topics Power Electron.*, vol. 5, no. 4, pp. 1631-1656, Dec. 2017.

[4] E. Solas, G. Abad, J. A. Barrena, S. Aurtenetxea, A. Cárcar, and L. Zajac, "Modular multilevel converter with different submodule concepts-Part I: Capacitor voltage balancing method," *IEEE Trans. Ind. Electron.*, vol. 60, no. 10, pp. 4525-4535, October 2013.

[5] S. Du, B. Wu and N. Zargari, "Common-mode voltage elimination for variable-speed motor drive based on flying-capacitor modular multilevel converter," *IEEE Trans. Power Electron.*, 2017, accepted.

[6] F. Ma, Z. He, Q. Xu, A. Luo, L. Zhou and M. Li, "Multilevel power conditioner and its model predictive control for railway traction system," *IEEE Trans. Ind. Electron.*, vol. 63, no. 11, pp. 7275-7285, Nov. 2016.

[7] T. Nakanishi, J. Itoh, "High Power Density Design for a Modular Multilevel Converter With an H-Bridge Cell Based on a Volume Evaluation of Each Component," *IEEE Trans. Power Electron.*, vol. 33, no. 3, pp. 1967-1984, Mar. 2018.

[8] F. Richardeau and T. Pham, "Reliability calculation of multilevel converters: theory and applications," *IEEE Trans. Ind. Electron.*, vol. 60, no. 10, pp. 4225-4233, Oct. 2013.

[9] H. Liu, P. C. Loh, and F. Blaabjerg, "Review of fault diagnosis and fault-tolerant control for modular multilevel converter of HVDC," in *Proc. IECON*, 2013, pp. 1242-1247.

[10] S. Shao, P. Wheeler, J. Clare, and A. Watson, "Fault detection for modular multilevel converters based on sliding mode observer," *IEEE Trans. Power Electron.*, vol. 28, no. 11, pp. 4867-4872, Nov. 2013.

[11] F. Deng, Z. Chen, M. K. Rezwan, and R. Zhu, "Fault detection and localization method for modular multilevel converters," *IEEE Trans. Power Electron.*, vol. 30, no. 5, pp. 2721-2732, May, 2015.

[12] B. Li, S. Shi, B. Wang, G. Wang, W. Wang, and D. Xu, "Fault diagnosis and tolerant control of single IGBT open-circuit failure in modular multilevel converters," *IEEE Trans. Power Electron.*, vol. 31, no. 4, pp. 3165-3176, Apr. 2016

[13] A. Ghazanfari and Y. A-R I. Mohamed, "A resilient framework for fault-tolerant operation of modular multilevel converters," *IEEE Trans. Ind. Electron.*, vol. 63, no. 5, pp. 2669-2678, May 2016.

[14] Q. Yang, J. Qin, and M. Saeedifard, "Analysis, detection, and location of open-switch submodule failures in a modular multilevel converter," *IEEE Trans. Power Del.*, vol. 31, no. 1, pp. 155-164, Feb. 2016.

[15] R. Picas, J. Zaragoza, J. Pou, S. Ceballos, "Reliable Modular Multilevel Converter Fault Detection With Redundant Voltage Sensor," *IEEE Trans. Power Electron.*, vol. 32, no. 1, pp. 39-51, Jan. 2017

[16] F. Deng, R. Zhu, D. Liu, Y. Wang, H. Wang, Z. Chen, M. Cheng, "Protection Scheme for Modular Multilevel Converters Under Diode Open-Circuit Faults," *IEEE Trans. Power Electron.*, vol. 33, no. 4, pp. 2866-2877, Apr. 2018

[17] S. Du, B. Wu and N. R. Zargari, "A Startup Method for Flying-Capacitor Modular Multilevel Converter (FC-MMC) With Effective Damping of LC Oscillations," *IEEE Trans. Power Electron*., vol. 32, no. 7, pp. 5827-5834, Jul. 2017

[18] M. Schnarrenberger, F. Kammerer, D. Bräckle, M. Braun, "Cell design of a square-wave powered 1AC-3AC modular multilevel converter low voltage prototype," in *Proc. EPE* 2016, pp. 1-11.

[19] V. Najmi, J. Wang, R. Burgos, D. Boroyevich, "High reliability capacitor bank design for modular multilevel converter in MV applications," in *Proc. ECCE* 2014, pp. 1051-1058.

[20] T. Nakanishi, J. Itoh, "Evaluation for overall volume of capacitor and heat-sink in step-down rectifier using modular multilevel converter," in *Proc. ECCE* 2015, pp. 1-10.

[21] Q. Wang, M. Cheng, Y. Jiang, W. Zuo and G. Buja, "A simple active and reactive power control for applications of single-phase electric springs," *IEEE Trans. Ind. Electron.*, vol. 65, no. 8, pp. 6291-6300, Aug. 2018.

[22] J. Yun-jae, N. Thanh Hai, and L. Dong-Choon, "Condition monitoring of submodule capacitors in modular multilevel converters," in *Proc. ECCE* 2014, pp. 2121-2126.

[23] O. Abushafa, S. Gadoue, M. Dahidah, and D. Atkinson, "A new scheme for monitoring submodule capacitance in modular multilevel converter," in *Proc. PEMD* 2016, pp. 1-6.

[24] F. Deng, D. Liu, Y. Wang, Z. Chen, M. Cheng and Q. Wang, "Capacitor monitoring for modular multilevel converters," in *Proc. IECON* 2017, pp. 934-939.

[25] R. Picas, J. Pou, J. Zaragoza, A. Watson, G. Konstantinou, S. Ceballos and J. Clare, "Submodule power losses balancing algorithms for the modular multilevel converter," in *Proc. IECON* 2016, pp. 5064-5069.

[26] P. Hu, R. Teodorescu, S. Wang, S. Li and J. M. Guerrero, "A currentless sorting and selection based capacitor-voltage-balancing method for modular multilevel converters," *IEEE Trans. Power Electron.*, In press, 2018.

[27] A. Dekka, B. Wu, V. Yaramasu, and N. R. Zargari, "Dual-stage model predictive control with improved harmonic performance for modular multilevel converter," *IEEE Trans. Ind. Electron*., vol. 63, no. 10, pp. 6010-6019, Oct. 2016.

[28] Q. Tu, Z. Xu and L. Xu, "Reduced switching-frequency modulation and circulating current suppression for modular multilevel converters," *IEEE Trans. Power Del.*, vol. 26, no. 3, pp. 2009-2017, Jul. 2011.

[29] X. Li, Q. Song, W. Liu, S. Xu, Z. Zhu and X. Li, "Performance analysis and optimization of circulating current control for modular multilevel converter," *IEEE Trans. Ind. Electron*., vol. 63, no. 2, pp. 716-727, 2016.

This article has been accepted for publication in a future issue of this journal, but has not been fully edited. Content may change prior to final publication. Citation information: DOI 10.1109/TPEL.2018.2857832, IEEE Transactions on Power Electronics

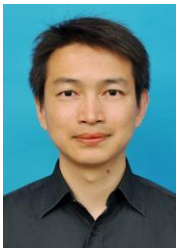

Fujin Deng (S'10-M'13) received the B.Eng. degree in electrical engineering from China University of Mining and Technology, Jiangsu, China, in 2005, the M.Sc. Degree in electrical engineering from Shanghai Jiao Tong University, Shanghai, China, in 2008, and the Ph.D. degree in energy technology from the Department of Energy Technology, Aalborg University, Aalborg, Denmark, in 2012.

He joined the Southeast University in 2017 and is currently a Professor in the School of Electrical Engineering, Southeast University, Nanjing, China. From 2013 to 2015 and from 2015 to 2017, he was a Postdoctoral Researcher and an Assistant Professor, respectively, in the Department of Energy Technology, Aalborg University, Aalborg, Denmark. His main research interests include wind power generation, multilevel converters, high-voltage direct-current technology, DC grid and offshore wind farm-power systems dynamics.

Qingsong Wang (S'14-M'17-SM'17) received the B.Sc. and M.Sc. degrees from the Department of Electrical Engineering, Zhejiang University, Hangzhou, China, in 2004 and 2007, respectively, and the Ph.D. degree from the School of Electrical Engineering, Southeast University, Nanjing, China, in 2016. From November 2015 to November 2016, he was a joint Ph.D student with the Department of Energy Technology, Aalborg University, Aalborg, Denmark, where he focused on electric springs.

From July 2004 to July 2005, he was an engineer in Shihlin Electronic & Engineering Co., Ltd, Suzhou, China. From July 2007 to August 2011, he was an engineer in Global Development Center of Philips Lighting Electronics, Shanghai, China. In October 2010, he was promoted to be a Senior Engineer. From August 2011 to September 2013, he was a Lecturer in PLA University of Science and Technology, Nanjing, China. Since 2017, he has been with Southeast University, where he is currently a Lecturer in the School of Electrical Engineering.

Dr. Wang's research interests are focused in the areas of control and applications of power electronics to power systems, smart grid, and lighting drivers.

Dong Liu (S'15-M'18) received the B.Eng. and an M.Sc. in electrical engineering from South China University of Technology, Guangzhou, China, in 2008 and 2011, and the Ph.D. degree in energy technology from the Department of Energy Technology, Aalborg University, Aalborg, Denmark, in 2018.

From 2011 to 2014, he was an R&D engineer in Emerson Network Power Co., Ltd., Shenzhen, China. From May, 2017 to November, 2017, he was a visiting scholar at the Center for Power Electronics Systems (CPES), Virginia Polytechnic Institute and State University, Blacksburg, VA, USA. His main research interests include renewable energy technology, multilevel converters, and DC/DC converters.

Yanbo Wang (S'15-M'17) was born in Gansu province, China, in 1986. He received the M.S. degrees in electrical engineering in the Electrical Engineering School, Southwest Jiaotong University, Chengdu, China, in 2011, and received Ph.D degree in the department of Energy Technology, Aalborg University, Denmark in 2017. Currently, he is with the department of Energy Technology in Aalborg University as a Postdoctoral Fellow. From June to October of 2016, he was a visiting scholar in Power System Research Group of the Department of Electrical and Computer Engineering, University of Manitoba, Winnipeg, MB, Canada. His research interests include stability analysis and control of power electronic-dominated power system, distributed power generation system and active distribution network.

Ming Cheng (M'01-SM'02-F'15) received the B.Sc. and M.Sc. degrees from the Department of Electrical Engineering, Southeast University, Nanjing, China, in 1982 and 1987, respectively, and the Ph.D. degree from the Department of Electrical and Electronic Engineering, The University of Hong Kong, Hong Kong, in 2001.

Since 1987, he has been with Southeast University, where he is currently a Distinguished Professor in the School of Electrical Engineering and the Director of the Research Center for Wind Power Generation. His teaching and research interests include electrical machines, motor drives for electric vehicles, and renewable energy generation. He has authored or coauthored over 300 technical papers and four books and is the holder of 55 patents in these areas.

Prof. Cheng is a fellow of the Institution of Engineering and Technology. He has served as chair and organizing committee member for many international conferences. He is a Distinguished Lecturer of the IEEE Industry Applications Society (IAS) in 2015/2016.

Zhe Chen (M'95-SM'98) received the B.Eng. and M.Sc. degrees all in Electrical Engineering from Northeast China Institute of Electric Power Engineering, Jilin City, China, MPhil in Power Electronic, from Staffordshire University, England and the Ph.D. degree in Power and Control, from University of Durham, England.

Dr Chen is a full Professor with the Department of Energy Technology, Aalborg University, Denmark. He is the leader of Wind Power System Research program at the Department of Energy Technology, Aalborg University and the Danish Principle Investigator for Wind Energy of Sino-Danish Centre for Education and Research.

His research areas are power systems, power electronics and electric machines; and his main current research interests are wind energy and modern power systems. He has led many research projects and has more than 400 technical publications with more than 10000 citations and h-index of 44 (Google Scholar).

Dr Chen is an Associate Editor of the IEEE Transactions on Power Electronics, a Fellow of the Institution of Engineering and Technology (London, U.K.), and a Chartered Engineer in the U.K.